

Laser-Based Patterning of Gold Nanoparticles into Microstructures

J. Xu,[†] J. Drelich,* and E. M. Nadgorny[‡]

Department of Materials Science and Engineering and Department of Physics,
Michigan Technological University, Houghton, Michigan 49931

Received April 29, 2003. In Final Form: December 10, 2003

A novel laser beam guided patterning technique for deposition of nanoparticle clusters of various materials on movable substrates and fabrication of microstructures is described. An example of the technique's application, the fabrication of gold microstrips of under 100–150 μm in width, is discussed. Microstrip patterning is achieved by making use of gold thiolate nanoparticles (7–20 nm). The experiments reveal one of the assets of this technique, the in situ manufacturing ability to form gold electrodes on deposited patterns. Such features could be explored for the fabrication of microsensors of varying conducting characteristics.

Introduction

The need for and popularity of chemical and biological microsensors have created a requirement for new techniques that could pattern organic and biological particles and molecules at microscopic and submicroscopic resolutions and scales without losing their chemical and biological activity. Photolithography and electron-beam lithography are the most popular patterning techniques, which are at the heart of modern-day microfabrication, nanotechnology, and molecular electronics. All such techniques require a resistive film and harsh chemical etching, which makes them unsuitable for patterning nanoparticles or molecules with organic or biological functionalities, since it causes destruction of organic molecules and biological entities.^{1–4} Other newly developed techniques, for example, such as “dip-pen nanolithography”, allow direct transporting and patterning of particles and molecules onto a substrate from the atomic force microscope (AFM) tip on a nanometer scale (~ 30 – 100 nm).¹ However, such techniques can usually convey only a small amount of materials, since their transfer efficiency is relatively low. Microcontact printing, which uses an elastomer stamp, can fabricate heterogeneous structures of micron-size and larger dimensions, but it has a limited potential for a mixed functionality surface fabrication.³ Additional limitations of these and many other patterning techniques are their incapability to produce structures and patterns of various composition. As a complement to many existing micro- and nanopatterning techniques, we describe in this Letter a novel patterning method that relies on guidance and deposition of particles by a laser beam, which we call the laser-based particle deposition (LBPD) technique. The main feature of the LBPD technique is that it guides and patterns nanoparticles of gold and other materials onto substrates, producing structures with a high specific surface area.

The LBPD technique exploits optical forces to control micron-sized droplets of liquid suspensions with nanoparticles inside a laser beam, so that the droplets are axially confined and propelled forward until they move through a small aperture to be deposited on a substrate.^{5–7} Unlike a similar technique developed before at Michigan Tech, which uses a hollow fiber to guide the droplets,^{8,9} LBPD not only significantly reduces the problem of hollow fiber clogging but also utilizes the near-field features of the aperture-diffracted laser beam. Like the other laser-based deposition technique, LBPD allows transporting a wide variety of materials, including metals, insulators, polymers, liquid droplets, and biomaterials, for final deposition and patterning on substrates.^{5–10} Another advantage of LBPD is its versatility of patterning different inorganic, organic, and biological materials on the same substrate. Complex structures have been formed by repeatedly depositing particles with sizes ranging from under 10 nm to several micrometers on translated substrates of different kinds. Due to prominent properties and flexibility afforded by the LBPD technique, it is envisioned that this technique (or its modification) could be adopted to fabricate microscopic and submicroscopic structures for chemical and biological microsensors of high sensitivity and selectivity.

Laser-Based Particle Deposition

The basic LBPD apparatus (Figure 1) consists of mist, source, and process chambers and a laser system. An

* Corresponding author. E-mail: jwdrelic@mtu.edu. Phone: 906-487-2932. Fax: 906-487-2934.

[†] Current address: BioForce Nanosciences, Inc., Ames, Iowa.

[‡] Department of Physics.

(1) Piner, R. D.; Zhe, J.; Xu, F.; Hong, S.; Mirkin, C. A. *Science* **1999**, *283*, 661.

(2) Madou, M. *Fundamentals of Microfabrication*; CRC Press: Boca Raton, FL, 1997.

(3) Kumar, H. A.; Biebuyck, H. A.; Whitesides, G. M. *Langmuir* **1994**, *10*, 1498.

(4) Urban, G. *Sens. Actuators, A: Phys.* **1999**, *A74*, 219.

(5) Xu, J.; Zhou, Ch.; Grant, S.; Nadgorny, E.; Drelich, J. In *Functional Nanostructured Materials Through Multiscale Assembly and Novel Patterning Techniques*; Moss, S. C., Ed.; MRS Symposium Proceedings; Materials Research Society: Pittsburgh, PA, 2002; Vol. 728, p S7.6.1.

(6) Drelich, J.; Nadgorny, E. M.; Zellers, E. T.; Xu, J.; Zhou, Ch.; White, C. L.; Cross, W. M. In *Functional Fillers and Nanoscale Minerals*; Kellar, J. J., Herpfer, M. A., Moudgil B. M., Eds.; MME Society Proceeding: Littleton, CO, 2003; pp 85–94.

(7) Nadgorny, E. M.; Zhou, Ch.; Drelich, J.; Zahn, R. In *Rapid Prototyping Technologies*; Holmes, A. S., Pique, A., Dimos, D. B., Eds.; MRS Symposium Proceedings; Materials Research Society: Pittsburgh, PA, 2003; Vol. 758, p LL4.4.1.

(8) Renn, M. J.; Pastel, R.; Lewandowski, H. J. *Phys. Rev. Lett.* **1999**, *82*, 1574.

(9) Renn, M. J.; Marquez, G.; King, B. H.; Essien, M.; Miller, W. D. In *Direct-Write Technologies for Rapid Prototyping Applications*; Pique, A., Chrisey, D. B., Eds.; Academic Press: New York, 2002; pp 475–492.

(10) Nadgorny, E. M.; Pastel, P. L.; Struthers, A. A.; Miner, A. In *Mass and Charge Transport in Inorganic Materials: Fundamental to Devices*; Vincenzini, P., Buscaglia, V., Eds.; Techna: Faenza, 2000; pp 1107–1114.

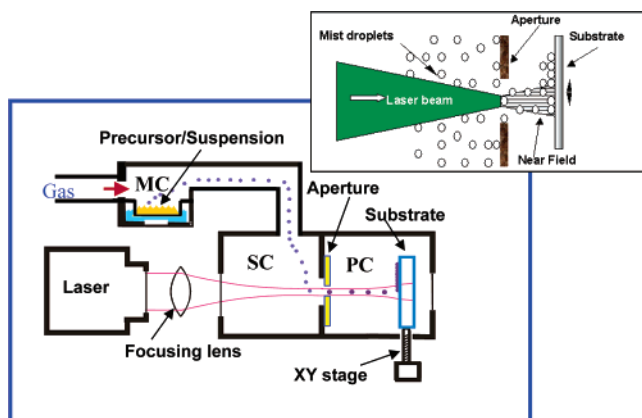


Figure 1. Schematic of the laser-based particle deposition (LBDP) apparatus: source of droplets/particles (nebulizer, carrier gas supply, and the mist chamber MC); supply (SC) and process (PC) chambers linked by a high-power laser aperture (details shown in the offset); laser system (532-nm YAG laser and focusing lenses); movable substrate on an *XY* stage.

ultrasonic nebulizer in the mist chamber produces a mist of submicron-sized liquid droplets from colloidal suspensions or precursors. A moderately intense laser beam directed along the axis of the aperture guides and transports the droplets from the source to the process chamber. Reactions in precursor droplets, if desired, can be initiated by the laser beam in-flight or on the deposit, producing a new material. The aperture orifice diameter is significantly larger than the transported droplets, and the strong focusing effect of the diffracted beam allows the controllable patterning of micron-sized lines.

There are several laser-induced forces acting on the droplets during the deposition process.^{7–12} Axial forces, known as the radiation pressure and the radiometric force, arise from scattering of light by the droplets and from droplet temperature gradients due to laser illumination, respectively. The axial forces propel droplets forward along the path of the laser beam. The transverse gradient force is a result of polarization of droplets in the nonuniform optical field of a Gaussian laser beam and confines the droplets to the high intensity region along the axis of the laser beam. The drag force of the medium against the forward motion of the droplets additionally stabilizes their axial position. (Some additional details are provided in a note in the reference list.¹¹) In the course of deposition inside the process chamber, the droplets are guided along precise trajectories for several hundred microns after leaving the aperture. These features enable conformal particle deposition on the substrate and, by translating the substrate, high-resolution patterning. More details on optical forces involved in deposition of particles by a laser beam are provided elsewhere.¹²

(11) Optical forces, radiometric forces, and drag force are three major forces that are essential for the droplet guidance in the LBDP technique. The optical forces are comprised of the radiation and gradient forces. The gradient (or confining) force arises from electrical forces exerted on a polarizable particle and can be calculated as $F_g = (\alpha/2)\nabla E^2$, where α is the particle polarizability and ∇E is the laser electric field gradient. The radiation (or forward) force can be calculated as $F_z = (\pi R^2 I_0 Q_{pr})/c$, where R is the particle radius, I_0 is the axial intensity of the laser beam, Q_{pr} is the efficiency for the radiation pressure, and c is the velocity of light in free space. The main radiometric force can be calculated as $F_r = (3\pi\eta^2 R_g R \Delta T)/pM$, where η is the ambient shear viscosity, R_g is the molar gas constant, ΔT is the temperature gradient inside the droplet, p is the pressure, and M is the molecular weight of the gas. The drag force is described by Stoke's formula, $F_D = 6\pi\eta Rv$, where v is the particle velocity. A more detailed description of the forces exerted by a laser beam on transported droplets is presented in ref 12.

(12) Nadgorny, E. M.; Drelich, J. In *Encyclopedia of Nanoscience and Nanotechnology*; Marcel Dekker: in press.

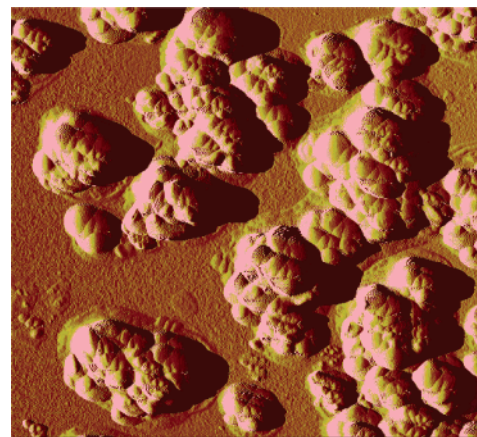


Figure 2. \times AFM image ($10 \times 10 \mu\text{m}^2$; the amplitude mode) of clusters made of 20-nm $\text{C}_6\text{H}_5(\text{CH}_2)_2\text{S-Au}$ nanoparticles deposited at a laser power of 100 mW on a glass substrate.

As mentioned, the LBDP technique allows axial guiding of particles from a nebulizer to substrate. Other well-known laser-based trapping techniques, often called the optical tweezers, make use of a strongly focused laser beam with a very strong axial gradient to allow axial trapping.¹³ This difference illustrates the main advantage of the LBDP technique over the optical tweezers: its ability to direct nanoparticles from various particle sources onto substrates to “write” on them and produce desirable structures.

In principle, virtually any material that is suspended in a liquid or formed by decomposition of a precursor liquid can be deposited by the LBDP technique. The principle limitations of the technique are that some precursors may undergo unwanted reactions (e.g. premature decomposition) inside the laser beam and that the substrate is not overheated by the incident laser beam. As demonstrated in the presented experiments, a proper choice of the wavelength of laser light can counter both of the problems.

Microstructures Constructed with Gold Nanoparticles

Gold nanoparticles coated with organic or biological functionality are finding promising application for chemical sensors¹⁴ and biosensors.¹⁵ In our study, the LBDP technique is employed for patterning gold thiolate ($\text{CH}_3(\text{CH}_2)_7\text{S-Au}$ and $\text{C}_6\text{H}_5(\text{CH}_2)_2\text{S-Au}$) nanoparticles from toluene suspensions to produce microstructures of different shapes and sizes. Figure 2 shows randomly distributed clusters of 20-nm gold thiolate nanoparticles on a substrate deposited during an early stage of the transporting process. The experiments demonstrated that the size, distribution, and shape of the deposited clusters depend on many factors, such as the size of carrying droplets generated by the nebulizer, the concentration, wettability, and other materials properties of nanoparticles in the liquid droplet, optical parameters of the laser beam, and wetting characteristics of the substrate in use, although detailed correlations between these variables still remain to be determined.

The shape of the irregular clusters shown in Figure 2 is primarily affected by the solvent (toluene in this case) used as a liquid carrier of the gold nanoparticles. Since toluene has a strong affinity for the thiolate moieties (2-ethylphenylsulfide) self-assembled on the gold surface,

(13) Ashkin, A. *Phys. Rev. Lett.* **1970**, *24*, 156–159.

(14) Cai, Q.-Y.; Zellers, E. T. *Anal. Chem.* **2002**, *74*, 3533.

(15) Bashir, R. *Mater. Today* **2001**, *11/12*, 30.

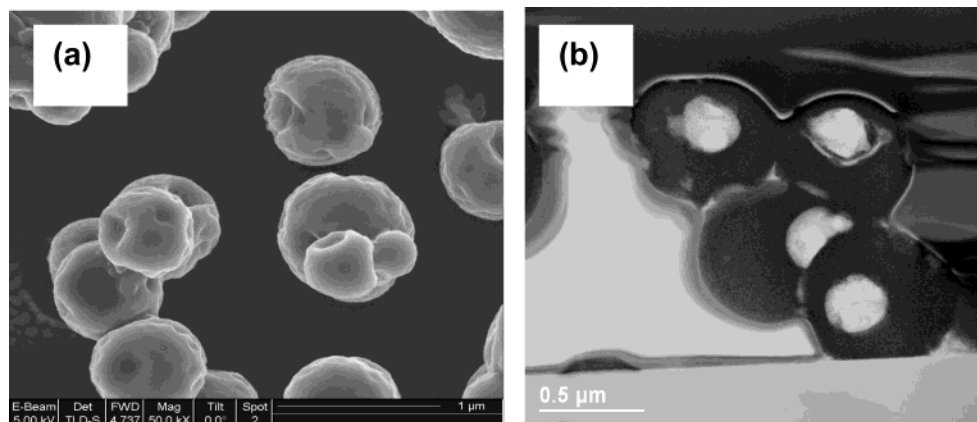


Figure 3. Structures formed by 7-nm hydrophobic Au–S(CH₂)₇CH₃ particles deposited at a laser power of 200 mW on glass: (a) scanning electron micrograph of microspheres; (b) transmission electron micrograph of the partially sectioned microspheres. The bright area in the middle of the clusters is where the cut was made, and the increased brightness reflects a reduced amount of gold nanoparticles in this sectioned area.

the particles remain dispersed in the toluene droplets instead of accumulating at the liquid–air interface. Droplets that carry nanoparticles dispersed in the liquid phase are expected to form less regular clusters on substrates than droplets coated with a monolayer of nanoparticles.¹² Our preliminary observations indicate that the wetting characteristics of the substrate also influence the shape of the deposited cluster. In particular, in the example shown in Figure 2, toluene remaining in the deposited clusters causes them to spread nonuniformly over the substrate surface. We further speculate that a nanoscale inhomogeneity of the substrate affects nonuniform spreading of deposited wet clusters into irregular shapes in Figure 2. Possible temperature gradients resulting from nonuniform heating of the substrate and the deposit itself by the laser beam can also have an impact on such surface spreading.

A higher concentration of nanoparticles in droplets entering the process chamber combined with complete (or almost complete) evaporation of the solvent lead to different, more regular shapes of spherical clusters, as shown in Figure 3a. As seen, individual overlapping spheres made of 7-nm gold particles are formed during deposition. Their size varies from about 0.1 to 1 μm, and their diameter is a direct consequence of both the size distribution of the nanoparticle-in-liquid droplets generated by the nebulizer and, to a lesser degree, the nanoparticles concentration in the droplets. The hydrophobic gold nanoparticles pack together, producing stable microstructures as a result of the interparticle van der Waals forces.

The transmission electron micrograph shown in Figure 3b reveals that the spheres are less filled inside, as indicated by a bright area of the sectioned spheres. Such an inhomogeneity reduces the strength of fabricated microstructures and causes a partial collapse of the shells. As a result, small undulations are formed, as can be seen in Figure 3a.

The formation of such shells is assumed to be a result of combined effects of liquid evaporation and capillarity phenomena. Indeed, when the laser beam heats a liquid droplet, evaporation progresses easily through the outer surface of the droplet. Evaporation is also initiated on the surface of nanoparticles inside the droplet via nucleation and growth of nanobubbles. As long as the concentration of the nanoparticles in the droplet is low, the bubbles can easily escape to the droplet surface. This is not the case, however, when a denser structure of the nanoparticles is created inside the droplet, resulting in fine porosity

through particle-to-particle alignment. A dense monolayer of hydrophobic gold nanoparticles is probably forming on the surface of the droplets soon after the droplet generation in early stages of the deposition process. Due to a high capillary pressure, the gaseous bubbles cannot pass through such a dense configuration of nanoparticles without disrupting its structure. It is possible to estimate such a pressure using the simplified Young–Laplace equation, $\Delta P = 2\gamma/R$, where γ is the surface tension of the liquid and R is the radius of the capillary opening. The result shows that a very high pressure of about 280 atm is required to force the gaseous–toluene interface to move through a capillary opening of 4 nm in diameter.

As discussed by Haw et al.,¹⁶ the drying of deposited nanoparticle-in-liquid droplets is a very complex process involving the interplay of mass and heat flow, time dependent rheological variations, and phase changes. Considering that the LYPD deposition includes additional thermal effects due to material–light interactions, the drying processes become even more complicated. The control of the morphology of clusters made of nanoparticles during the spray drying has recently been achieved through understanding and control of hydrodynamic effects in this process.¹⁷ Understanding the clusters drying processes during the laser beam-guided transportation and deposition process could also lead to better deposited structures on the micro- or submicroscale.

Multiple depositions of gold nanoparticles over the same area allowed us to form a variety of more-or-less uniform dense structures, with a thickness in the range from $<1\ \mu\text{m}$ to $>20\ \mu\text{m}$ and with lateral dimensions in the range from about 20 to 150 μm in width and up to a few centimeters in length. Figure 4 shows a gold microstrip of densely packed 7-nm CH₃(CH₂)₇S–Au particles produced by a prolonged deposition. As seen, the particles form a dense strip with small local variation in thickness but individual spheres of clustered particles can still be observed on the top of the dense layer (Figure 4b). A comparison between Figures 4 and 2 suggests that in the first stage of the transporting process individual clusters are deposited on a substrate but then they disintegrate to a dense layer during the subsequent deposition. A transition from clusters to a two-dimensional structure might result from the spreading effects initiated by residual toluene in the deposited clusters.

(16) Haw, M. D.; Gillie, M.; Poon, W. C. K. *Langmuir* **2002**, *18*, 1626.
(17) Iskandar, F.; Gradon, L.; Okuyama, K. *J. Colloid Interface Sci.* **2003**, *265*, 296.

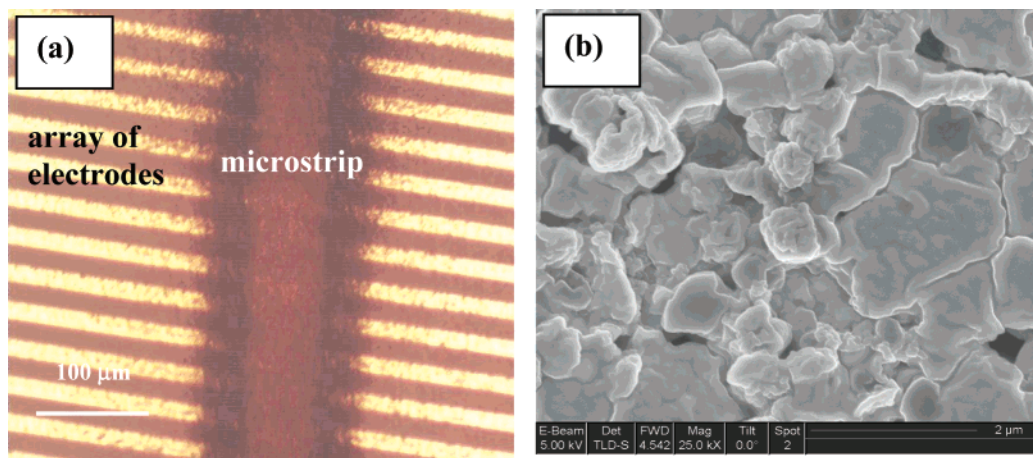


Figure 4. Highly dense gold vertical microstrip of $\sim 100 \mu\text{m}$ in width and $15\text{--}20 \mu\text{m}$ in thickness made of 7-nm $\text{CH}_3(\text{CH}_2)_7\text{S}\text{--Au}$ particles deposited over an array of gold microelectrodes on a quartz substrate. The pictures represent an optical image (a) and a $2 \times 2 \mu\text{m}^2$ scanning electron micrograph (b).

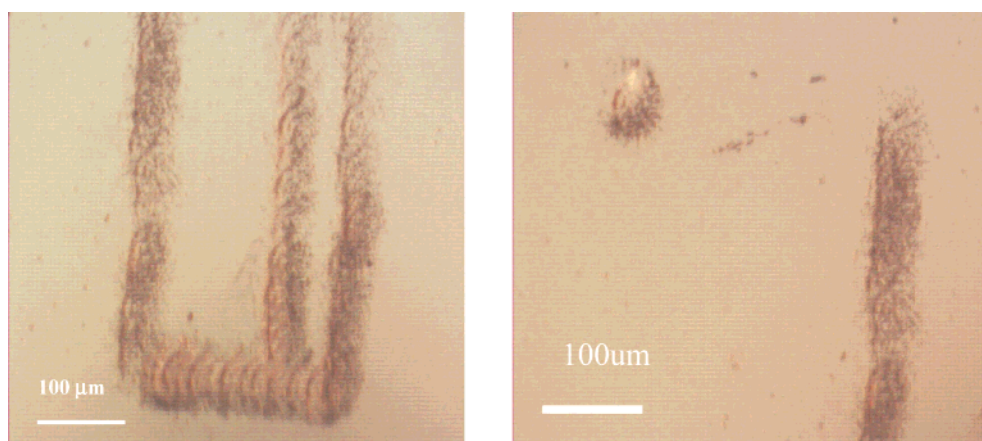


Figure 5. Optical images of microstructures made of 20-nm $\text{C}_6\text{H}_5(\text{CH}_2)_2\text{S}\text{--Au}$ nanoparticles as deposited on a glass substrate. The thickness of the structures is $< 5 \mu\text{m}$.

Depositing polystyrene nanoparticles allows us to pattern microstrips as narrow as $2 \mu\text{m}$, but gold microstrips under $20 \mu\text{m}$ have not been produced yet with the current set of apertures ($> 20 \mu\text{m}$ in diameter). A higher absorption of gold particles might be one of the reasons for such different behavior, requiring a further study of material property effects. Obviously, higher accuracy and control over the dimensions of the patterned structures are essential for the success of the proposed novel direct-write technique. As preliminary results revealed, many factors affect the patterning precision and rate, including mist formation and flow, size and population of droplets, mist supply system design, laser beam dimensions and focus, transport distance, ratio of beam waist diameter to the size of the aperture, optical properties of particles, and alignment and parameters of the laser beam, and further studies will show if confident control over the deposition precision and rate can be achieved in this technique.¹²

As demonstrated in Figure 5, the LBPDP technique also opens up new possibilities to the fabrication of multiple arrays and microstructures of complex geometry. The left image shows three parallel gold strips, from 55 to $65 \mu\text{m}$ in width, distanced by about 30 and $100 \mu\text{m}$, and connected at a base. The right image shows a gold circle of $70 \mu\text{m}$ in about $200 \mu\text{m}$ from a $50\text{--}\mu\text{m}$ -wide gold strip. A limited uniformity of the structures shown in Figure 5 results from manual manipulation of the substrate position. Motorized substrate displacement will provide a better control of deposited structures and will broaden the versatility of the deposited shapes.

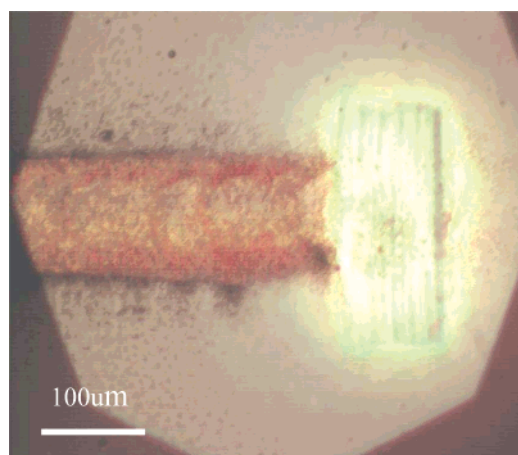


Figure 6. Microstrip ($\sim 120\text{-}\mu\text{m}$ wide) made of 7-nm $\text{CH}_3\text{--}(\text{CH}_2)_7\text{S}\text{--Au}$ nanoparticles, with gold electrodes produced by in situ melting. The thickness of the microstrip is $> 5 \mu\text{m}$.

One of the important features of the LBPDP technique is its in situ ability to thermally process the deposited materials and structures. In particular, increasing the laser power allows us to melt gold particles during or after deposition. As a result, selected parts of the patterned structure can be converted into solid gold electrodes as shown in Figure 6. Such capabilities of the LBPDP technique in nanoparticles deposition offer strong possibilities of fabricating novel microsensing devices with functionalities

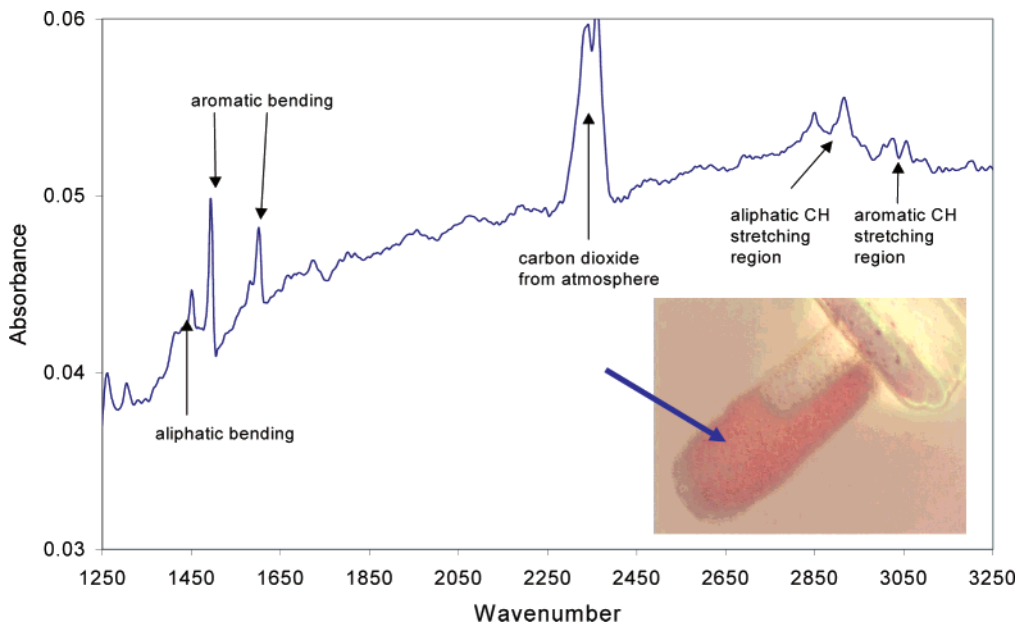


Figure 7. FTIR spectrum from a $C_6H_5C_2H_4$ -Au array deposited using a 532-nm laser at a power of 100 mW. The spectrum was acquired by the UMA 500 IR microscope with a Digilab FTS-600 spectrometer using the micro-ATR technique with a germanium element.⁶ The optical picture in the lower right corner is an image of the ~ 100 - μm -wide array with the arrow indicating the IR analysis area.

that can be controlled by changing the conducting characteristics of various portions of a manufactured microsensor.

Another important feature of the LBPD technique is its ability to preserve organic/biological functionalities on the surface of the patterned metal nanoparticles, which is critical for many applications, such as manufacturing chemical and biological microsensors. Since all particles, including gold, absorb laser light, the induced thermal effects might degrade organic/biological assemblies attached to the metal nanoparticles. The preservation of surface organic functionality of deposited and patterned gold nanoparticles often represents a crucial step in manufacturing densely integrated arrays of chemical and/or biological functionalities for recognition and quantification of pollutants.

As demonstrated,⁶ such a problem has been solved by using a laser intensity as low as ≤ 100 mW during the deposition. This is illustrated by the FTIR spectrum of

Figure 7: original aliphatic and aromatic bending of the $C_6H_5C_2H_4SH$ on gold nanoparticles is retained not only after deposition but also after additional local in situ melting to produce the end electrodes. Since the absorption of gold nanoparticles strongly depends on the wavelength,¹⁸ the use of lasers of different wavelengths in the near-infrared region could substantially reduce unwanted thermal effects in the deposition processes of gold and other particles.

Acknowledgment. The authors would like to express their appreciation to Elvin Beach and Steve Rozeveld of Dow Chemical Company for scanning electron microscopy and transmission electron microscopy images. The gold thiolate nanoparticles were received from E. T. Zellers of the University of Michigan.

LA0347253

(18) Mulvaney, P. *MRS Bull.* **2001**, 26, 1009.